CHEMISTRY OF MATERIALS
Article

Chem. Mater. **2009,** *21,* 5691–5694 5691
DOI:10.1021/cm9020172

Atomic Layer Deposition of Hexagonal and Orthorhombic $YMnO_3$ Thin Films

K. Uusi-Esko, J. Malm, and M. Karppinen*

Laboratory of Inorganic Chemistry, Department of Chemistry, Helsinki University of Technology, P.O. Box 6100, FI-02015 TKK, Finland

Received July 6, 2009. Revised Manuscript Received October 14, 2009

Thin films of both the hexagonal and orthorhombic forms of $YMnO_3$ have been fabricated through atomic layer deposition (ALD) and subsequent heat treatment. ALD-type growth of essentially cation-stoichiometric $YMnO_3$ films was achieved in a reproducible manner in a temperature interval of 250−300 °C using $Y(thd)_3$, $Mn(thd)_3$, and ozone as precursors. The as-deposited films were amorphous, but a postdeposition heat treatment carried out in a temperature range of 750−900 °C depending on the substrate/polymorph yielded highly crystalline films. On Si(100) substrate, the product was the hexagonal phase of $YMnO_3$, whereas on $LaAlO_3$(100) and $SrTiO_3$(100) substrates, the metastable orthorhombic $YMnO_3$ phase was formed. On the perovskite substrates, the films were highly oriented, the direction of the orientation moreover depending on the choice of the substrate crystal.

1. Introduction

Manganese oxides of the general formula $RMnO_3$ (R = rare-earth element) are a versatile group of materials hosting interesting phenomena such as colossal magnetoresistance and multiferroic effects.[1−7] The $RMnO_3$ system is divided into two subsystems with rather different crystal structures whose relative stabilities are mainly determined by the size of the R^{III} cation. For the larger rare earths, R = La−Dy, an orthorhombically distorted perovskite structure (*Pbnm*) is adopted, i.e. o-$RMnO_3$, whereas for the smaller rare earths, R = Sc, Y, and Ho−Lu, the structure is hexagonal ($P6_3cm$), i.e. h-$RMnO_3$, under normal synthesis conditions.[8,9] Metastable perovskites of the smaller Rs were prepared for the first time in the 1960s through high-pressure high-temperature conversion.[10] Although the fabrication becomes increasingly difficult as the size of the rare-earth element decreases, the entire $RMnO_3$ series of metastable perovskites has been prepared under high pressures.[10−14] Epitaxial phase stabilization is another practical tool that can be used to obtain many metastable oxides in spite of their thermodynamic instability in bulk form. Stabilization of metastable phases as thin films is based on free-energy gain due to structural coherence at the film/substrate interface. It has been utilized in the fabrication of metastable $RMnO_3$ compounds by radio-frequency magnetron sputtering,[15,16] pulsed laser deposition,[16,17] and metal-organic chemical vapor deposition.[18]

Atomic layer deposition (ALD) has earlier been used to deposit thin films of only a few ternary manganites: (La,Ca)MnO_3, (La,Sr)MnO_3, and $ZnMnO_3$.[19−23] ALD is

*Corresponding author. Phone: +358-9-470-22600. Fax: +358-9-462 373. E-mail: maarit.karppinen@tkk.fi.

(1) Bertaut, E. F.; Forrat, E. F.; Fang, P. H. *C. R. Acad. Sci. Paris* **1963**, *265*, 1958.
(2) Hwang, H. Y.; Cheong, S.-W.; Radaelli, P. G.; Marezio, M.; Batlogg, B. *Phys. Rev. Lett.* **1995**, *75*, 914.
(3) Von Helmolt, R.; Wecker, J.; Holzapfel, B.; Schultz, L.; Samwer, K *Phys. Rev. Lett.* **1993**, *71*, 2331.
(4) Huang, Z. J.; Cao, Y.; Sun, Y. Y.; Xue, Y. Y.; Chu, C. W. *Phys. Rev. B* **1997**, *56*, 2623.
(5) Fiebig, M.; Lottermosser, Th.; Fröhlich, D.; Goltsev, A. V.; Pisarev, R. V. *Nature* **2002**, *419*, 818.
(6) Kimura, T.; Goto, T.; Shintani, H.; Ishizaka, K.; Arima, T.; Tokura, Y. *Nature* **2003**, *426*, 55.
(7) Yen, F.; dela Cruz, C.; Lorenz, B.; Galstyan, E.; Sun, Y. Y.; Gospodinov, M.; Chu, C. W. *J. Mater. Res.* **2007**, *22*, 2163.
(8) Yakel, H. L.Jr. *Acta Crystallogr.* **1955**, *8*, 394.
(9) Yakel, H. L.Jr.; Koehler, W. C.; Bertaut, E. F.; Forrat, F. *Acta Crystallogr.* **1963**, *16*, 957.
(10) (a) Waintal, A.; Capponi, J. J.; Bertraut, E. F.; Contré, M.; François, D. *Solid State Commun.* **1966**, *4*, 125. (b) Waintal, A.; Chevanas, J. *Mater. Res. Bull.* **1967**, *2*, 819.
(11) Huang, Y. H.; Fjellvåg, H.; Karppinen, M.; Hauback, B. C.; Yamauchi, H.; Goodenough, J. B. *Chem. Mater.* **2006**, *18*, 2130.
(12) Zhou, J.-S.; Goodenough, J. B.; Gallardo-Amores, J. M.; Morán, E.; Alario-Franco, M. A.; Caudillo, R. *Phys. Rev. B* **2006**, *74*, 14422.
(13) Imamura, N.; Karppinen, M.; Fjellvåg, H.; Yamauchi, H. *Solid State Commun.* **2006**, *140*, 386.
(14) Uusi-Esko, K.; Malm, J.; Imamura, N.; Yamauchi, H.; Karppinen, M. *Mater. Chem. Phys.* **2008**, *112*, 1029.
(15) Fujimura, N.; Ishida, T.; Yoshimura, T.; Ito, T. *Appl. Phys. Lett.* **1996**, *69*, 1011.
(16) Fujimura, N.; Azuma, S.; Aoki, N.; Yoshimura, T.; Ito, T. *J. Appl. Phys.* **1996**, *80*, 7084.
(17) Salvador, P. A.; Doan, T.-D.; Mercey, B.; Raveau, B. *Chem. Mater.* **1998**, *10*, 2592.
(18) Bosak, A. A.; Kamenev, A. A.; Graboy, I. E.; Antonov, S. V.; Gorbenko, O. Yu.; Kaul, A. R.; Dubourdieu, C.; Senator, J. P.; Svechnikov, V. L.; Zandbergen, H. W.; Holländer, B. *Thin Solid Films* **2001**, *400*, 149.
(19) Nilsen, O.; Rauwel, E.; Fjellvåg, H.; Kjekshus, A. *J. Mater. Chem.* **2007**, *17*, 1466.
(20) Nilsen, O.; Peussa, M.; Fjellvåg, H.; Niinistö, L.; Kjekshus, A. *J. Mater. Chem.* **1999**, *9*, 1781.
(21) Wojcik, A.; Kobalko, K.; Godlewski, M.; Lusakowska, E.; Paszkowicz, W.; Dybko, K.; Domagala, J.; Szczerbakow, A.; Kaminska, E. *Acta Phys. Pol., A* **2004**, *105*, 667.
(22) Mantovan, R.; Georgieva, M.; Perego, M.; Lu, H. L.; Cocco, S.; Zenkevich, A.; Scarel, G.; Fanciulli, M. *Acta Phys. Pol., A* **2007**, *112*, 1271.
(23) Holme, T. P.; Lee, C.; Prinz, F. B. *Solid State Ionics* **2008**, *179*, 1540.

Published on Web 11/11/2009

a gas-phase technique in which precursor vapors are pulsed alternately into the reaction chamber and the thin film growth proceeds through surface reactions in a self-limiting manner. The growth mechanism and the sequential pulsing of precursors lead to the various attractive features of ALD including excellent conformality, simple and accurate thickness control (growth per cycle), relatively easy scale-up, and good uniformity on large areas.[24] With ALD, high-quality thin films can be produced even on three-dimensional structures[25] making it a highly desirable technique for the microelectronics industry. Growth of ternary oxides by ALD is generally challenging compared to the rather straightforward deposition of binary oxides. First, suitable and compatible precursors need to be found for each of the metals, and furthermore, the cation stoichiometry has to be accurately controlled in order to achieve the desired material reproducibly. In this study, we have successfully deposited cation-stoichiometric $YMnO_3$ thin films by ALD and demonstrated the role of the substrate material in determining the resultant crystal structure.

2. Experimental Section

Thin films of $Y_xMn_yO_3$ were deposited in a commercial flow-type ALD reactor (F-120 by ASM Microchemistry Ltd.). Metal precursors $Y(thd)_3$ and $Mn(thd)_3$ (thd = 2,2,6,6-tetramethylheptane-3,5-dionate) were synthesized according to methods described in refs. 26 and 27 and purified by sublimation. Ozone was produced by feeding oxygen gas (99.999%) to the reactor through an ozone generator (Fischer model 502). The concentration of ozone was ca. 10% (60 g/m^3), and the gas flow rate during the pulse was about 60 cm^3/min (measured for the oxygen gas). Nitrogen (>99.999%, Schmidlin UHPN 3000 N_2 generator) was used as a carrier and purging gas. The metal precursors were evaporated inside the reactor from open glass crucibles held at 123 °C. The yttrium and manganese precursor pulsing times were 1.5 and 2 s, respectively. The metal precursor pulses were followed by equally long N_2 pulses. The ozone pulsing time was 1.5 s followed by a N_2 purge of 2 s. A few tests were also performed with varying the pulsing and purging times. The pulsing and purging times did not cause any notable difference in the composition or the growth rate of the films in the temperature interval 250−300 °C, but a slight increase in the growth rate was observed at the highest temperatures. The pulsing sequences were designed to maximize the probability of proper mixing of the components. The films were grown under a pressure of 2−3 mbar on Si(100), $LaAlO_3$(100) (pseudocubic, a = 3.79 Å),[28] and $SrTiO_3$(100) (cubic, a = 3.91 Å) substrates. Most of the films were grown on 5 × 5 cm^2 silicon substrates positioned vertically inside the reactor chamber. The smaller substrates were attached with metal clips to 5 × 5 cm^2 pieces of soda-lime glass mounted in a vertical position. The depositions were performed in the temperature interval 250−350 °C, chosen based on earlier studies.[19,29] The lower limit is set by the slow growth of Y_2O_3 at temperatures below 250 °C, and the upper limit is close to the highest usable temperature (330 °C) for $Mn(thd)_3$ in the growth of ternary manganese oxide films. Above 325 °C, the film quality started to decline and thickness variations were observed. As the optimum film thickness depended on the characterization method used, films with thicknesses between 55 and 220 nm were deposited. Selected samples were heat-treated in a rapid-thermal-annealing (RTA) furnace (PEO 601, ATV Technologie GmbH). Annealing was carried out in N_2 atmosphere for 10 min at temperatures between 600 and 1000 °C.

Phase identification was performed by X-ray diffraction (XRD) measurements with a Philips MPD 1880 powder diffractometer using Cu Kα1 radiation (equipped with diffracted beam and secondary monochromators). The Y:Mn ratio was determined by X-ray fluorescence (XRF) spectrometer (Philips PW 1480 WDS) using Rh excitation. Data were analyzed with the UNIQUANT 4.34 program which utilizes a DJ Kappa model to calculate simultaneously the composition and the mass thickness of an unknown bulk or thin film sample.[30] Film thicknesses were determined by fitting of reflectance spectra recorded with a Hitachi U-2000 double beam spectrophotometer in the wavelength region of 190−1100 nm. Thicknesses of selected samples were also determined by X-ray reflection (XRR) and spectrophotometric ellipsometry (Picometer Ellipsometer, Beaglehole Instruments). The XRR measurements were carried out with a Philips X'pert Pro diffractometer operating with Cu Kα1 radiation. It was concluded that the absolute values obtained using the spectrophotometer were slightly larger compared to the two other techniques. However, there was only a minor increase in the error with increasing thickness. Thus, the values obtained using the spectrophotometer could be used to compare growth rates at different temperatures and with different precursor pulsing sequences.

3. Results and Discussion

The $Y_xMn_yO_3$ films grown in the temperature range of 250−325 °C were in general uniform in appearance with no apparent decrease in thickness toward the edges of the 5 × 5 cm^2 silicon substrate. Above 325 °C, the film quality started to decline and thickness variations could be observed. In Figure 1, the temperature dependence of the $YMnO_3$ deposition rate and the Mn content against the total metal content, i.e. y:($x + y$), is shown for films grown with a cation pulsing ratio Y:Mn = 1:1. A small trend toward increasing Mn content can be observed. In the temperature range 250−300 °C, the growth rate does not vary significantly, but a slight increase in the growth rate can be observed at 325 °C. In earlier studies, the growth of

(24) Putkonen, M.; Sajavaara, T.; Niinistö, L.; Keinonen, J. *Anal. Bioanal. Chem.* **2005**, *382*, 1791.
(25) Ritala, M.; Leskelä, M. *Handbook of Thin Film Materials*; Nalwa, H. S., Ed.; Academic Press: San Diego, 2002; Vol. *1*, Atomic layer deposition, p 103.
(26) Eisentraut, K. J.; Sievers, R. E. *J. Am. Chem. Soc.* **1956**, *87*, 5254.
(27) Hammond, G. S.; Nonhebel, D. C.; Wu, C.-H. S. *Inorg. Chem.* **1963**, *2*, 73.
(28) Geller, S.; Bala, V. B. *Acta Crystallogr.* **1956**, *9*, 1019.
(29) Putkonen, M.; Sajavaara, T.; Johansson, L.-S.; Niinistö, L. *Chem. Vap. Deposition* **2001**, *7*, 44.
(30) UniQuant Version 2 User Manual; Omega Data Systems: Veldhoven, The Netherlands, **1994**.

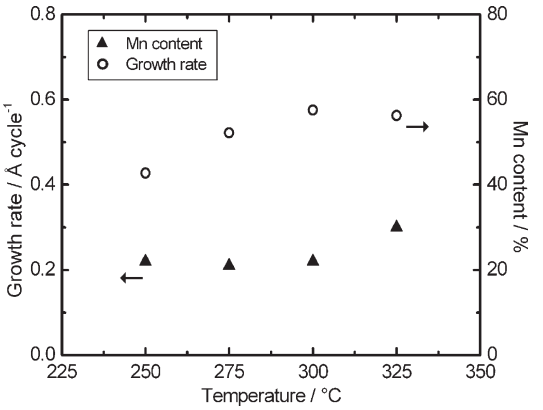

Figure 1. Growth rate and Mn content (against the total metal content, i.e. y:($x + y$)) as a function of temperature for $Y_xMn_yO_3$ films prepared with a Y:Mn pulsing ratio of 1:1.

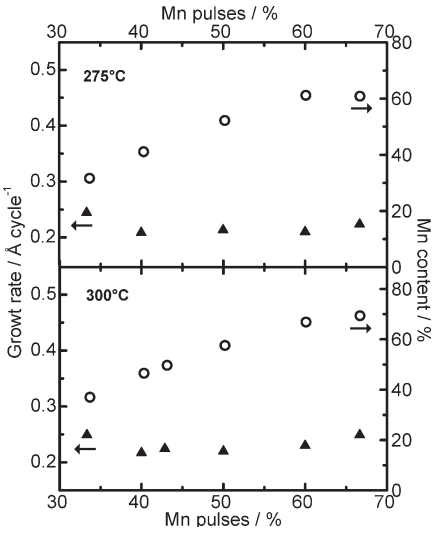

Figure 2. Effect of the pulsing fraction of $Mn(thd)_3$ on the Mn content and on the growth rate of $Y_xMn_yO_3$ films at deposition temperatures of 275 and 300 °C. Open symbols refer to film composition and filled symbols refer to growth rate.

the binary oxide MnO_x has been found to become uncontrolled due to the decomposition of $Mn(thd)_3$ above 240 °C.[31] However, in the cases of $LaMnO_3$ and $CaMnO_3$,[19] the stability of $Mn(thd)_3$ was greatly enhanced enabling the growth of ternary oxides even at 330 °C. Such enhanced stability was clearly observed in the present study as well such that thin films of $YMnO_3$ with rather constant growth rate could be deposited in the temperature interval 250−300 °C. The existence of a temperature interval with constant growth rate is often considered as a criterion for ALD-type growth.

The effect of the Y:Mn pulsing ratio on the composition and the growth rate of $Y_xMn_yO_3$ films deposited at 275 and 300 °C is demonstrated in Figure 2. According to the XRF analyses, the Mn content, y:($x + y$), of the films deposited on silicon was nearly linearly dependent on the pulsing ratio with only a slight deviation at a pulsing ratio Y:Mn = 1:2. Pulsing ratios with the highest Mn pulse

(31) Nilsen, O.; Fjellvåg, H.; Kjekshus, A. *Thin Solid Films* **2003**, *444*, 44.

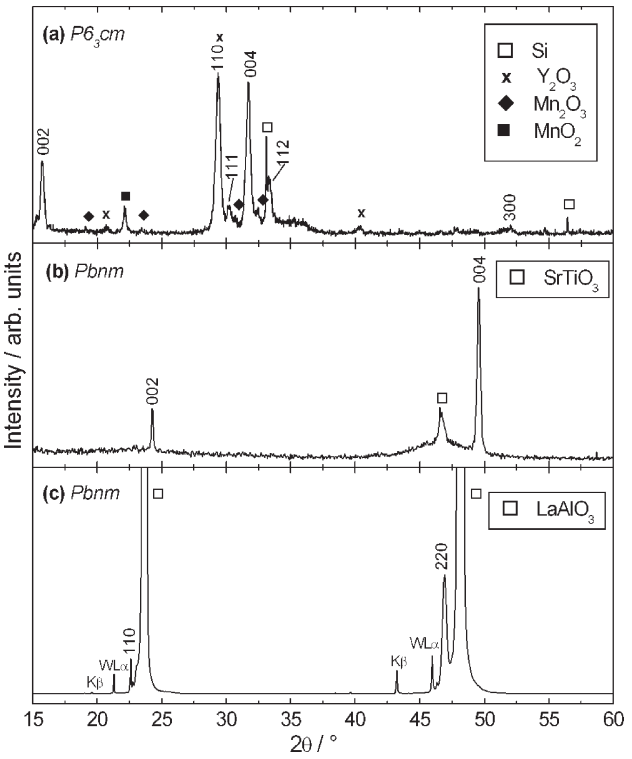

Figure 3. XRD patterns of annealed (at 1000 °C in N_2 flow) $YMnO_3$ films deposited on (a) Si(100), (b) $SrTiO_3$(100), and (c) $LaAlO_3$(100). The indices are for the hexagonal space group $P6_3cm$ in (a) and for the orthorhombic space group *Pbnm* in (b) and (c).

numbers, e.g. Y:Mn = 1:7, led to substantial decrease in the film quality. Since these films contain an excess of Mn, the observation is in good accordance with the fact that the deposition of MnO_x becomes uncontrolled at temperatures above 240 °C.[31] Due to the linear dependency between the number of Mn pulses and the Mn content of the films, it was easy and straightforward to deposit a film with the desired Y:Mn ratio. The film stoichiometry was maintained while increasing the film thickness verifying the surface-controlled nature of the process.

All the as-deposited $YMnO_3$ films were amorphous regardless of the substrate or the composition of the film. Hexagonal $YMnO_3$ started to crystallize at 900 °C (Figure 3a) when stoichiometric films grown on silicon substrates were annealed in N_2 flow. On the other hand, annealing nonstoichiometric films with metal ratios Y:Mn = 0.44 and 1.70 did not result in the formation of h-$YMnO_3$ in any of the cases irrespective of the annealing temperature or the cooling rate. Stoichiometric films deposited on $LaAlO_3$ and $SrTiO_3$ substrates began to crystallize at 750 °C resulting in single-phase films of the metastable orthorhombic $YMnO_3$ perovskite phase. The perovskite structure is formed instead of the hexagonal one due to epitaxial stabilization of the phase on the perovskite substrates with low lattice mismatch. The average lattice mismatch is 1.85% on $SrTiO_3$ substrate and 1.26% on $LaAlO_3$ substrate.[18] Orthorhombic $YMnO_3$ was highly oriented on both $LaAlO_3$ and $SrTiO_3$ substrates (Figures 3b and 3c). On $LaAlO_3$, the orientation was observed in the [110] direction, and on $SrTiO_3$,

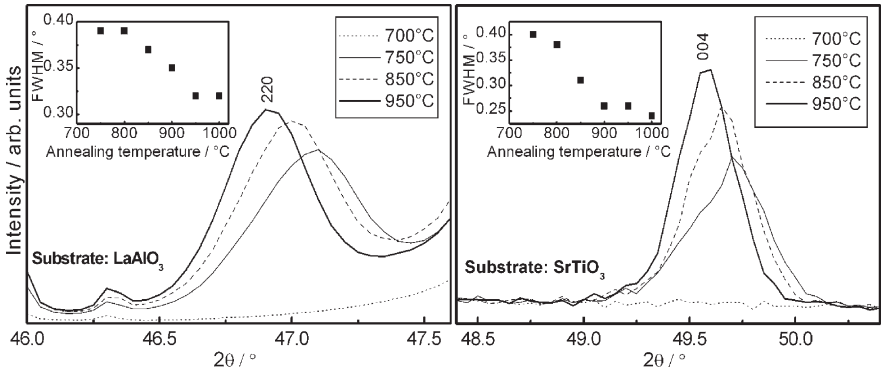

Figure 4. Selected sections of XRD patterns of annealed (at different temperatures in N_2 flow) $YMnO_3$ films deposited on $LaAlO_3$ (left) and $SrTiO_3$ (right) substrates. The insets show the change in FWHM values as a function of annealing temperature.

Table 1. Annealing Temperatures, *d* Spacings, and FWHM Values of $YMnO_3$ Films Deposited on $LaAlO_3$ (220 Reflection) and $SrTiO_3$ (004 Reflection) Substrates

	$LaAlO_3$		$SrTiO_3$	
annealing temperature/°C	*d* spacing/Å	FWHM/deg	*d* spacing/Å	FWHM/deg
750	1.930	0.39	1.834	0.40
800	1.931	0.39	1.836	0.38
850	1.932	0.37	1.837	0.31
900	1.935	0.35	1.838	0.26
950	1.937	0.32	1.839	0.26
1000	1.937	0.32	1.839	0.24

in the [001] direction. According to the full width at half-maximum (FWHM) values, the crystallinity improved with increasing annealing temperature (Figure 4, Table 1).

Interestingly, as seen in Figure 4 and in Table 1, a tiny but systematic shift was observed in the 2θ values of the diffraction peaks of o-$YMnO_3$ as a function of the annealing temperature. Such behavior could be caused by stress release at the substrate-film interface for instance through adjustment of the oxygen stoichiometry as was suggested by Nilsen et al.[19] in the case of (La,Ca)-MnO_3 thin films. However, in contrast to the (La,Ca)-MnO_3 system, the oxygen stoichiometry of $YMnO_3$ is not easily altered. In our case, the 2θ values decrease with increasing annealing temperature indicating an increase in at least one of the unit-cell parameters. However, this does not necessarily mean there is an increase in the unit-cell volume, which could be caused by an oxygen loss from the structure. Considering this and the fact that any changes in the oxygen stoichiometry of $YMnO_3$ are unlikely, it is clear that understanding the shifting of the diffraction peaks with increasing annealing temperature requires further investigation.

4. Conclusions

Both hexagonal and orthorhombic $YMnO_3$ were fabricated as thin films through ALD and post-deposition heat treatment. The crystal structure of the films and, in the case of orthorhombic $YMnO_3$, even the direction of the orientation could be controlled simply by the choice of the substrate crystal. An ALD window was found in the temperature range of 250−300 °C within which the growth rate and the film composition remained essentially constant. The film stoichiometry was maintained while increasing the film thickness demonstrating the good surface-controlled nature of the process.

The as-deposited films were amorphous and a post-deposition heat treatment was needed to crystallize the films. Hexagonal $YMnO_3$ was formed on silicon substrates after annealing stoichiometric films at 900 °C in N_2 flow. The formation of metastable orthorhombic $YMnO_3$ was successfully promoted by depositing amorphous $YMnO_3$ thin films on coherent perovskite substrates. Orthorhombic $YMnO_3$ started to crystallize at 750 °C on both $LaAlO_3$ and $SrTiO_3$ substrates. The crystallinity of h-$YMnO_3$ and o-$YMnO_3$ films improved clearly with increasing annealing temperature up to 1000 °C. For the highly oriented o-$YMnO_3$ films, this effect was shown by the decreasing FWHM values.

Acknowledgment. This work was supported by Academy of Finland (nos. 114517, 116254, and 126528) and Finnish Foundation for Technology Promotion. The authors are indebted to M.Sc. M. Bosund (Department of Micro and NanoSciences, Helsinki University of Technology) for XRR measurements and to Dr. K. Yliniemi (Laboratory of Physical Chemistry, Department of Chemistry, Helsinki University of Technology) for ellipsometry measurements.